IκB-ζ Expression Requires Both TYK2/STAT3 Activity and IL-17–Regulated mRNA Stabilization

Ryuta Muromoto, Keisuke Tawa, Yui Ohgakiuchi, Ami Sato, Yuka Saino, Koki Hirashima, Hiroya Minoguchi, Yuichi Kitai, Jun-ichi Kashiwakura, Kazuya Shimoda, Kenji Oritani and Tadashi Matsuda

ImmunoHorizons 2019, 3 (5) 172-185
doi: https://doi.org/10.4049/immunohorizons.1900023
http://www.immunohorizons.org/content/3/5/172

ImmunoHorizons is an open access journal published by
The American Association of Immunologists, Inc.,
1451 Rockville Pike, Suite 650, Rockville, MD 20852

ISSN 2573-7732.

ImmunoHorizons

RESEARCH ARTICLE

Innate Immunity

IκB-ζ Expression Requires Both TYK2/STAT3 Activity and IL-17–Regulated mRNA Stabilization

Ryuta Muromoto,* Keisuke Tawa,* Yui Ohgakiuchi,* Ami Sato,* Yuka Saino,* Koki Hirashima,* Hiroya Minoguchi,* Yuichi Kitai,* Jun-ichi Kashiwakura,* Kazuya Shimoda,† Kenji Oritani,‡ and Tadashi Matsuda*

*Department of Immunology, Graduate School of Pharmaceutical Sciences, Hokkaido University, Sapporo 060-0812, Japan; †Department of Internal Medicine II, Faculty of Medicine, University of Miyazaki, Kiyotake, Miyazaki 889-1692, Japan; and ‡Department of Hematology, International University of Health and Welfare, Narita, Chiba 286-8686, Japan

ABSTRACT

Cytokine IL-17A (IL-17) acts on various cell types, including epidermal keratinocytes, and induces antimicrobial peptide and chemokine production to elicit antibacterial and antifungal defense responses. Excess IL-17 leads to inflammatory skin diseases such as psoriasis. The IκB family protein IκB-ζ mediates IL-17–induced responses. However, the mechanism controlling IκB-ζ expression in IL-17–stimulated cells remains elusive. In this study, we showed that JAK kinase TYK2 positively regulates IL-17–induced IκB-ζ expression. TYK2-deficient mice showed reduced inflammation and concomitant reduction of IκB-ζ mRNA compared with wild-type mice in imiquimod-induced skin inflammation. The analysis of the IκB-ζ promoter activity using human cell lines (HaCaT and HeLa) revealed that catalytic activity of TYK2 and its substrate transcription factor STAT3, but not IL-17, is required for IκB-ζ promoter activity. In contrast, IL-17–induced signaling, which did not activate STAT3, posttranscriptionally stabilized IκB-ζ mRNA via its 3′-untranslated region. IL-17 signaling protein ACT1 was required to counteract constitutive IκB-ζ mRNA degradation by RNase Regnase-1. These results suggested that transcriptional activation by TYK2–STAT3 pathway and mRNA stabilization by IL-17–mediated signals act separately from each other but complementarily to achieve IκB-ζ induction. Therefore, JAK/TYK2 inhibition might be of significance in regulation of IL-17–induced inflammatory reactions. *ImmunoHorizons*, 2019, 3: 172–185.

INTRODUCTION

Psoriasis is an immune-related chronic skin disease characterized by erythematous, scaly, sharply demarcated plaques. On lesions, excessive proliferation of epidermal keratinocytes is observed with infiltration of neutrophils, macrophages, and activated T cells (1). IL-17A (IL-17) is a key inflammatory cytokine present within psoriasis lesions (2–4) and is mainly produced from immune cells, such as activated T cells. IL-17 has a direct effect on the induction of genes expressed by keratinocytes involved in innate immune defense and a range of CXC chemokines that regulate immune cell trafficking (5–7). This immune cell feedback has been considered to amplify and prolong psoriatic inflammation (2, 8). Biologic agents neutralizing IL-17 (i.e., secukinumab and ixekizumab) or antagonizing its receptor (i.e., brodalumab) are used as therapeutic drugs and show a high clinical efficacy for treating psoriasis (9). Elucidating the signaling mechanism of IL-17–induced

Received for publication March 20, 2019. Accepted for publication April 25, 2019.

Address correspondence and reprint requests to: Dr. Ryuta Muromoto and Prof. Tadashi Matsuda, Department of Immunology, Graduate School of Pharmaceutical Sciences, Hokkaido University, Kita-12 Nishi-6, Kita-ku, Sapporo 060-0812, Japan. E-mail addresses: muro@pharm.hokudai.ac.jp (R.M.) and tmatsuda@pharm.hokudai.ac.jp (T.M.)

ORCIDs: 0000-0002-7474-493X (R.M.); 0000-0002-7863-6696 (J.-i.K.).

This work was supported by the Japan Society for the Promotion of Science KAKENHI (Grants 254600560, 17K08263, and 19H03364) and the Fugaku Trust for Medical Research.

Abbreviations used in this article: ChIP, chromatin immunoprecipitation; CHX, cycloheximide; Gluc, *Gaussia* luciferase; IκB-ζ-promoter-Luc, *NFKBIZ* promoter–luciferase reporter; IL-17, IL-17A; IMQ, imiquimod; KD, kinase domain; ΔKD, kinase domain–deleted TYK2; NHEK, normal human epidermal keratinocyte; qPCR, quantitative real-time PCR; siRNA, small interfering RNA; TSS, transcriptional start site; TYK2, tyrosine kinase-2; 3′UTR, 3′-untranslated region; WT, wild-type.

The online version of this article contains supplemental material.

https://doi.org/10.4049/immunohorizons.1900023

ImmunoHorizons is published by The American Association of Immunologists, Inc.

keratinocyte activation is important for understanding psoriasis pathogenesis.

Tyrosine kinase-2 (TYK2) is a JAK family kinase member and is activated in response to various cytokines, including type I IFNs (IFN-α/β), IL-12, and IL-23 (10–12). We previously reported that TYK2 deficiency attenuates imiquimod (IMQ)- and IL-23–induced ear thickening resulting from epidermal hyperplasia with inflammatory cell infiltration, suggesting that signals through TYK2 are required for psoriasis-like skin inflammation in mice (13, 14). Genome-wide association studies identified TYK2 as a psoriasis susceptibility gene (15–17). Because TYK2 is involved in IL-12/IL-23 signaling that activates IFN-γ/IL-17 production in T cells (12), suppression of psoriasis-like pathologic condition due to TYK2 deficiency has been mainly attributed to suppressed T cell activity (14, 18). It has not been sufficiently verified that TYK2 in keratinocytes may have a role in the IL-17 response, despite TYK2 protein expression in keratinocytes. In this study, we aimed to elucidate the role of TYK2 in the keratinocyte IL-17 response.

The IκB-ζ protein (also known as INAP or MAIL, encoded by *NFKBIZ*) is highly expressed in the epidermal keratinocytes of psoriatic lesions and is considered to be involved in psoriasis pathogenesis (19). The *NFKBIZ* gene is located in a psoriasis susceptibility locus on 3q12.3 (17). We have reported that IκB-ζ is an IL-17–inducible protein and mediates IL-17–induced gene expression (20). IκB-ζ is a nuclear IκB family protein that positively or negatively modulates NF-κB–dependent transcription depending on the cellular context (21). The contribution of IκB-ζ in the pathogenesis of IMQ-induced skin inflammation in mice seemed to be larger than the contribution of IL-17 (19), presumably because IκB-ζ has multiple induction pathways in addition to IL-17 signaling, as exemplified by other psoriasis-associated cytokines such as IL-17F, IL-1β, or IL-36 (22, 23). The transcriptional activator of IκB-ζ expression has been suggested to be transcription factors NF-κB (23, 24) and/or STAT3 (23, 25).

Signaling pathways activated by IL-17 control mRNA stability (26). The importance of IL-17–induced stabilization of mRNAs in inflammation, as well as its multiple mechanisms, has become increasingly evident (27–30). Regnase-1 (also known as MCPIP1, encoded by *ZC3H12A*) is the IL-17–inducible protein with endoribonuclease activity that acts as a negative feedback regulator for inflammatory signaling induced by TLR ligands or various cytokines, including IL-17 (31–35). Regnase-1 has been shown to be degraded rapidly through the ubiquitin–proteasome pathway in LPS-treated macrophages and activated T cells, as well as IL-17–, IL-1β–, or IL-36α–treated keratinocytes (33, 36–38). Stimulus-induced decrease of Regnase-1 protein levels has been considered to release a brake on mRNA expression. Recent studies have shown that the 3′-untranslated region (3′UTR) of IκB-ζ mRNA is required for the recognition, degradation, and/or translational suppression by Regnase-1 (39, 40). Altogether, these findings suggested that IL-17 signaling upregulates IκB-ζ through quantitative and/or qualitative inhibition of Regnase-1; however, this has not been sufficiently investigated.

In this study, we showed that TYK2 positively regulates IL-17–induced IκB-ζ expression in keratinocytes. TYK2-deficient mice showed decreased inflammation and concomitant reduction of IκB-ζ mRNA compared with wild-type (WT) mice in the IMQ-induced skin inflammation model. Small interfering RNA (siRNA)–mediated TYK2 knockdown reduced IL-17–induced expression of IκB-ζ and its target genes in keratinocytes. The TYK2–STAT3 pathway enhanced IκB-ζ promoter activity in a TYK2 kinase activity–dependent manner, but STAT3 phosphorylation was not enhanced by IL-17 stimulation. IL-17 stimulation posttranscriptionally stabilized IκB-ζ mRNA through Regnase-1 inhibition independently of TYK2. Our data showed that the activity of the TYK2–STAT3 pathway and IL-17–induced inhibition of Regnase-1 are regulated independently of each other, and both of them are required for IL-17–induced IκB-ζ upregulation.

MATERIALS AND METHODS

Plasmid construction and reagents

Human TYK2 cDNA was a gift from Dr. J. Ihle (St. Jude Children's Research Hospital, Memphis, TN). Full-length cDNA of TYK2, kinase-negative TYK2 (harboring a K930R mutation in the ATP-binding site), and the kinase domain–deleted TYK2 (ΔKD: aa 1–867) were generated by PCR and were subcloned into the pCS2-MT vector for mammalian expression. The plasmid expressing the TYK2 kinase domain (KD; aa 833–1187) was described previously (41). Expression vector for FLAG-tagged STAT3C, a constitutively active form of STAT3, has been described previously (42). The firefly luciferase reporter pGL3-mIκB-ζ (mNfkbiz)-3′UTR-Full (1–1353 nt after the stop codon), pFLAG-CMV2-mZc3h12a (mRegnase-1)-WT, and pFLAG-mZc3h12a (mRegnase-1)-D141N were kindly provided by Dr. O. Takeuchi (Kyoto University, Kyoto, Japan) (39). The mutant forms of Regnase-1 (C157A and D225/226A) were generated by site-directed mutagenesis. The pFN21A clone expressing an N-terminal HaloTag fusion of human full-length ACT1 (HaloTag-ACT1) was obtained from the Kazusa DNA Research Institute (Kisarazu, Japan). A fluorescent reporter construct, pCAG-mVenus-Nfkbiz-3′UTR, was generated in two steps: first, pCAG-mVenus was constructed from pCAG-YFP (43) (gift from C. Cepko; Addgene plasmid number 11180) by replacing YFP with the monomeric Venus coding sequence, which was obtained by cutting mVenus N1 (44) (gift from S. Vogel; Addgene plasmid number 27793) with restriction enzymes EcoRI and NotI. The 150-nt portion of mouse *Nfkbiz* 3′UTR after the stop codon, which contains two Regnase1-recognition stem-loops and plays a crucial role in mRNA stability (39), was inserted in the pCAG-mVenus downstream of the Venus gene using the In-Fusion HD cloning kit (Clontech). Stem-loop–disrupting mutations in the reporter plasmid were inserted by PCR. The secondary structures of the intact and mutated *Nfkbiz* 3′UTR mRNA were predicted by the CentroidFold Web server (45) (http://www.ncrna.org). Human *NFKBIZ* promoter–luciferase reporter (IκB-ζ-promoter-Luc; HPRM11632-PG04) was purchased from GeneCopoeia (Rockville, MD). This promoter clone simultaneously expresses naturally secreted *Gaussia* luciferase (Gluc) under the control of the promoter sequence (−1148 to +98) of *NFKBIZ* transcript variant

1 (NM_031419) and secreted alkaline phosphatase under the control of the CMV promoter, which serves as the internal control. The mutated promoter clones for each of two putative STAT-binding sites in the *NFKBIZ* promoter region were generated by PCR. All primers used for the plasmid constructions are listed in Supplemental Table I. Recombinant human IL-17 was purchased from R&D Systems (Minneapolis, MN). Cycloheximide (CHX), actinomycin D, and pyridone-6 were purchased from Wako Pure Chemical Industries (Osaka, Japan). Cerdulatinib was obtained from MedChem Express (Monmouth Junction, NJ). Tofacitinib/CP-690550 was obtained from Phoenix Pharmaceuticals (Burlingame, CA).

IMQ-induced skin inflammation

Tyk2$^{-/-}$ mice, BALB/c background, were described previously (13). Mice were kept under specific pathogen-free conditions and provided with food and water ad libitum. All experiments were performed according to the guidelines of the Institutional Animal Care and Use Committee of Hokkaido University. At 8–10 wk of age, mice received a daily topical dose of 10 mg of commercially available IMQ cream (5%, Beselna Cream; Mochida Pharmaceuticals, Tokyo, Japan) on the side of the ears for three consecutive days. To evaluate the severity of ear skin inflammation, affected ear thickness was measured. At the days indicated, ear thickness was measured using the thickness gauge (Mitutoyo, Kawasaki, Japan) and averaged. After application for three consecutive days, ears were collected for quantitative PCR analysis.

Cell culture and transfection of siRNA

Primary normal human epidermal keratinocytes (NHEKs) were purchased from KURABO (Tokyo, Japan) and cultured using the DermaLife K Comp Kit (KURABO). The human keratinocyte cell line HaCaT and the human cervix carcinoma cell line HeLa were maintained in DMEM containing 10% FCS. For siRNA transfection, the Lipofectamine 2000 reagent (Life Technologies, Carlsbad, CA) was used. The siRNAs targeting human *TYK2*, *ZC3H12A*, *TRAF3IP2*, and *STAT3* used in this study are purchased from Shanghai GenePharma (Shanghai, China) and are listed in Supplemental Table II.

RNA isolation and quantitative real-time PCR

Cells were harvested and total RNA was prepared using the TRI Reagent (Molecular Research Center, Cincinnati, OH). First-strand cDNA was synthesized from 1 μg of total RNA with ReverTra Ace (TOYOBO, Osaka, Japan). Quantitative real-time PCR (qPCR) analysis of transcripts was carried out using a combination of a KAPA SYBR FAST qPCR master mix (KAPA Biosystems, Woburn, MA) with a Mx3005P real-time PCR system (Stratagene, Santa Clara, CA). qPCR primers used in this study are listed in Supplemental Table I.

ELISA

IL-19 protein levels in culture supernatants of IL-17–treated cells were assayed by the Quantikine Human IL-19 Immunoassay kit according to the manufacturer's instructions (R&D Systems).

Luciferase assay for NFKBIZ promoter activity

HeLa cells were transfected with IκB-ζ-promoter-Luc, together with each expression vector for human TYK2, its kinase mutants (K930R, ΔKD, and KD), or a constitutively active form of STAT3 (STAT3C). At 24 h posttransfection, cells were treated with 100 ng/ml IL-17 and incubated for an additional 1.5 h. The culture supernatants were collected, and Gluc activities were measured using a Secrete-Pair Dual Luminescence Assay kit (GeneCopoeia) according to the manufacturer's instructions.

Luciferase and Venus reporter assays for posttranscriptional regulation of NFKBIZ mRNA

HeLa cells were transfected with luciferase reporter plasmid pGL3 containing the mouse *Nfkbiz* 3′UTR (full length: 1353 nt after the stop codon), together with the expression plasmid for human TYK2 or empty (control) plasmid. The gene encoding *Renilla* luciferase was transfected simultaneously as an internal control. After 24 h of cultivation, treatment with 100 ng/ml IL-17, and a subsequent 1.5 h of incubation, cells were lysed and luciferase activity in lysates was determined with the Dual-Luciferase Reporter Assay System (Promega, Madison, WI). The Venus reporter assay was conducted for further analysis. pCAG-mVenus-*Nfkbiz*-3′UTR (150 nt) or its stem-loop–disrupted mutant in the 3′UTR, together with each expression vector for Regnase-1, Regnase-1 mutants (D141N, C157A, or D225/226A), or ACT1, was introduced to HeLa cells. At 24 h posttransfection, cells were treated with 100 ng/ml IL-17 and incubated for an additional 1.5 h. The number of Venus-expressing cells, which is considered to reflect mRNA stabilization/degradation control through the 3′UTR, was counted using flow cytometry (FACSCalibur; Becton Dickinson), and the IL-17–induced fold change of the number of Venus-positive cells was calculated.

Immunoblotting

Immunoblotting was performed as described previously (46). Briefly, cell lysates were resolved on SDS-PAGE and transferred to PVDF transfer membranes (PerkinElmer, Boston, MA). The filters were then immunoblotted with each Ab. Immunoreactive proteins were visualized using an ECL detection system (Millipore, Bedford, MA). Anti–IκB-ζ (number 9244) and anti-TYK2 (number 9312) Abs were from Cell Signaling Technology (Beverly, MA); anti–β-defensin 2 (FL-64) and anti-STAT3 (C-20) Abs were from Santa Cruz Biotechnology (Santa Cruz, CA). Anti–Myc-tag (9E10) and anti-actin (AC15) Abs were from Sigma-Aldrich (St. Louis, MO); anti–phospho-STAT3 (Y705) Ab (EP2147Y) was from Abcam (Cambridge, U.K.).

Chromatin immunoprecipitation

HaCaT cells in a 6-cm dish were exposed to 10 μM cerdulatinib or DMSO for 1 h. Chromatin immunoprecipitation (ChIP) assays were performed as described previously (47), with some modifications. The Abs used in this study for immunoprecipitations were rabbit monoclonal anti-STAT3 Ab (79D7; Cell Signaling Technology) and normal rabbit IgG (negative control). After

incubation with the Ab, DNA–protein–Ab complexes were collected using Dynabeads M-280 Sheep Anti-Rabbit IgG (Thermo Fisher Scientific). Eluted DNA was analyzed by qPCR. The following sequence-specific ChIP qPCR primers were used to amplify two different NFKBIZ promoter regions: the promoter region upstream of transcriptional start site (TSS) 1 for NFKBIZ isoform 1 (NM_031419) and the TSS2 for NFKBIZ isoform 2 (NM_001005474) (Supplemental Table I). The promoter regions for TSS1 and TSS2 harbor putative STAT3-binding motifs. The negative-control primer was designed in an intronic region of the NFKBIZ gene lacking putative STAT3-binding motifs. Input DNA (5% of sample) was used as a control in each reaction. The relative ChIP amplification levels of each fragment were presented as percentages of total inputs in three experiments.

Statistical evaluation

Data are expressed as mean ± SEM. For statistical comparison of two groups, a Student *t* test was performed. For multiple comparisons, an ANOVA and Tukey test were conducted. A p value <0.05 was chosen as an indication of statistical significance.

RESULTS

Involvement of TYK2 in Nfkbiz expression in IMQ-induced psoriasis-like skin inflammation

We investigated the role of TYK2 in IκB-ζ gene expression in skin inflammation using TYK2-deficient mice. In psoriasis-affected skin, IL-17 produced by T cells induces neutrophil infiltration and production of antimicrobial peptides (such as β-defensins) from keratinocytes, thereby exacerbating psoriasis symptoms (48). We used a psoriasis-like skin inflammation model induced by topical application of an imidazoquinoline derivative, IMQ (49). As we reported earlier, by applying IMQ to the ear pinna of WT mice for three consecutive days (at days 0, 1, and 2), a significant auricular thickening was observed at days 2 and 3 (Fig. 1A). In contrast, application of IMQ to TYK2-deficient mice resulted in significant auricular thickening at day 3, but the degree was significantly milder than that of WT mice. The influence of TYK2 deficiency on the mRNA expression of IL-17–responsive genes IκB-ζ (*Nfkbiz*), *Il19*, and *Defb2* in the ear skin was examined. In IMQ-treated WT mice, expression of these IL-17–responsive genes was enhanced. In TYK2-deficient mice, IMQ application did not significantly increase IL-17–responsive genes (Fig. 1B). Of note, the level of *Il17a* mRNA in the IMQ-treated ears of TYK2-deficient mice was lower than in those of WT mice but was still firmly detected (Fig. 1B). These results suggested that TYK2 deficiency resulted in the decreased induction of IL-17–responding as well as IL-17 genes in the IMQ-treated lesions.

TYK2 promotes cellular responses to IL-17

IκB-ζ is important for IL-17–induced gene expression and inflammation, and we examined the role of TYK2 in *NFKBIZ* (encoding IκB-ζ) expression. The human *NFKBIZ* gene has two transcript variants driven by two distinct promoters (Fig. 2A). This

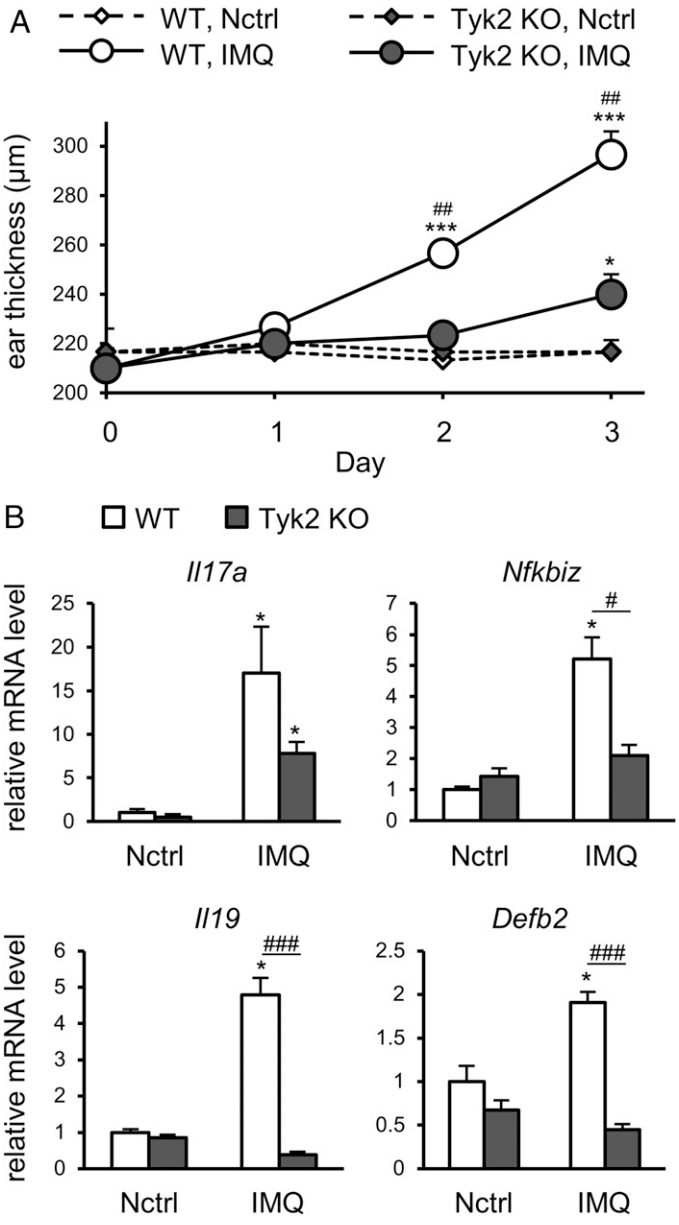

FIGURE 1. TYK2-deficient mice showed reduced inflammation and *Nfkbiz* expression in IMQ-induced skin inflammation.

(**A**) Ear skin of WT and Tyk2 knockout (KO) mice was treated with or without IMQ for three consecutive days. Ear swelling was evaluated by a dial thickness gauge on the days indicated. Plots show mean ± SEM of three to four mice per group from three independent experiments. (**B**) Effect of TYK2 deficiency on mRNA levels of IL-17–related genes (*Il17a*, *Nfkbiz*, *Il19*, and *Defb2*) in the ear skin 24 h after application of IMQ for three consecutive days. Plots show mean ± SEM of three to four mice per group from three independent experiments. $^{*}p < 0.05$, $^{***}p < 0.001$ compared with negative control (Nctrl); $^{\#}p < 0.05$, $^{\#\#}p < 0.01$, $^{\#\#\#}p < 0.001$ compared with Tyk2 KO.

feature and the overall gene structure of *NFKBIZ* are conserved between humans and mice (Supplemental Fig. 1). *NFKBIZ* transcript variant 1 (NM_031419), which is transcribed from the

TSS1, was upregulated at 1.5 h after IL-17 addition in control siRNA-transfected HaCaT cells. The induction was significantly attenuated in TYK2 siRNA-treated cells (Fig. 2A). *NFKBIZ* transcript variant 2 (NM_001005474), which is transcribed from the alternative TSS2 and has a slightly distinct mRNA sequence because of differential exon usage, was also induced by ~3-fold at 1.5 h after IL-17 addition, and it was not affected by TYK2 knockdown (Fig. 2A). These results suggested that transcript variant specificity exists in TYK2-mediated regulation of *NFKBIZ* expression. We have reported that IL-17–induced expression of *DEFB4A* and *IL19* is mediated by IκB-ζ (20). In TYK2-knockdown HaCaT cells, the IL-17–induced expression of these targets was reduced compared with control siRNA-treated cells (Fig. 2B). IL-17–induced secretion of IL-19 protein was significantly decreased by siRNA knockdown of TYK2 (Fig. 2C). Similar results showing TYK2 involvement in the IL-17 response were obtained in NHEKs (Fig. 2D) and HeLa cells (data not shown). Thus, TYK2 may have an effect on gene expression in keratinocytes and other cells responsive to IL-17.

Distinct roles for TYK2 function and IL-17–induced signaling in IκB-ζ induction

The mechanism of TYK2-mediated upregulation of IκB-ζ was investigated. First, a luciferase reporter plasmid expressed under the control of the promoter region sequence (−1198 to +98) upstream of the TSS1 of the IκB-ζ gene (IκB-ζ-promoter-Luc) was transiently introduced into HeLa cells (Fig. 3A). We investigated the effects of transient overexpression of TYK2 and IL-17 stimulation on transcriptional induction of IκB-ζ (Fig. 3B, 3C). The luciferase activity was significantly enhanced by TYK2 overexpression. In contrast, IL-17 did not activate the IκB-ζ-promoter-Luc. Next, we introduced plasmids expressing WT TYK2, kinase-inactive point mutant (K930R), kinase domain–deleted mutant (ΔKD), or the kinase domain (KD) into HeLa cells (Fig. 3D, 3E, 3F). In cells transfected with TYK2 K930R and TYK2 ΔKD, which do not have catalytic activity, IκB-ζ promoter activation was not induced (Fig. 3E). Overexpression of TYK2 KD was sufficient for enhancing IκB-ζ promoter activity. These results indicated that TYK2-mediated IκB-ζ-promoter activation depends on its kinase activity.

The 3′UTR downstream of the protein coding region of IκB-ζ mRNA affects IκB-ζ mRNA stability via regulatory stem-loop elements conserved to mammalian species including humans and mice (39). A reporter plasmid (IκB-ζ-3′UTR-Luc), in which a 3′UTR sequence derived from murine IκB-ζ mRNA was inserted downstream of a luciferase gene expressed under the constitutively active CMV promoter (39), was used to determine the effects of TYK2 overexpression and IL-17 stimulation (Fig. 3G, 3H, 3I). TYK2 overexpression did not affect 3′UTR-regulated reporter activity, whereas IL-17 stimulation showed a considerable enhancing effect (Fig. 3H). These data suggested that the TYK2-mediated signaling pathway is involved in the transcriptional regulation of IκB-ζ expression. IL-17 was found to primarily enhance the stability of IκB-ζ mRNA posttranscriptionally.

IL-17 signaling counteracts Regnase-1–mediated posttranscriptional mRNA degradation

Regarding the posttranscriptional mRNA stabilizing effect of IL-17 via the 3′UTR IκB-ζ mRNA sequence, our flow cytometric assay using the fluorescent protein (Venus)–based reporter fused to the truncated IκB-ζ 3′UTR (1–150 nt from stop codon) showed that this region of the IκB-ζ 3′UTR can respond to IL-17 stimulation (Fig. 4A, 4B). This region reportedly has two characteristic highly conserved stem-loop structures (denoted as "e" and "f" in Fig. 4A) that are required for the recognition, degradation, and/or translational suppression by an RNase, Regnase-1/MCPIP1 (encoded by *ZC3H12A*) (39, 40). The two stem-loops in the Venus-IκB-ζ 3′UTR reporter were mutated to disrupt these secondary structures (Fig. 4A). The loop-mutant reporter showed enhanced expression compared with the control intact reporter under unstimulated conditions, whereas it did not respond to IL-17 (Fig. 4B). Knockdown of endogenous Regnase-1 in HaCaTs or NHEKs by siRNA resulted in an accumulation of basal IκB-ζ mRNA levels, but it did not significantly affect IκB-ζ mRNA levels in IL-17–treated conditions (Fig. 4C). A recent study showing that IL-17 stimulation caused Regnase-1 protein degradation (33) has implied that the decrease of functional Regnase-1 protein could be a common mechanism between IL-17 stimulation and siZC3H12A for target mRNA stabilization. This overlapping mechanism would account for the nonsignificant effect of siZC3H12A on the accumulation of IκB-ζ mRNA, especially after IL-17 stimulation. Overexpression of either WT Regnase-1 or the C157A mutant, which lacks a deubiquitinase function but retains RNase activity (50), significantly suppressed Venus-IκB-ζ-3′UTR reporter expression (Fig. 4D), suggesting that the 3′UTR-mediated suppression is deubiquitinase-independent. The introduction of RNase-defective mutants of Regnase-1 (D141N and D225/226A) (36, 50) showed a possible dominant-negative effect on endogenous Regnase-1 and resulted in enhanced basal expression of the IκB-ζ-3′UTR reporter and unresponsiveness to IL-17 (Fig. 4D). These results suggested that Regnase-1–mediated degradation of IκB-ζ mRNA may occur constitutively and that the IL-17–induced signal may counteract Regnase-1–mediated mRNA degradation.

An IL-17 signaling adaptor protein, ACT1 (encoded by *TRAF3IP2*) (51), has been shown to mediate IL-17–induced upregulation of IκB-ζ mRNA in keratinocytes (17), although it is unclear whether ACT1 is required for IκB-ζ 3′UTR-mediated mRNA stabilization in IL-17–treated cells. We found that IL-17–induced expression of Venus-IκB-ζ-3′UTR reporter was abrogated by ACT1 knockdown (Fig. 4E). In addition, ACT1 overexpression counteracted the suppressing function of Regnase-1 on Venus-IκB-ζ-3′UTR reporter expression (Fig. 4F). These results suggested that IL-17/ACT1 signaling counteracts the constitutively occurring Regnase-1–mediated degradation of IκB-ζ mRNA.

Regnase-1 is considered to destabilize target mRNAs in a protein translation–dependent manner, as the translation inhibitor CHX can block mRNA decay mediated by Regnase-1 (39). Consistently, inhibition of the constitutive activity of Regnase-1

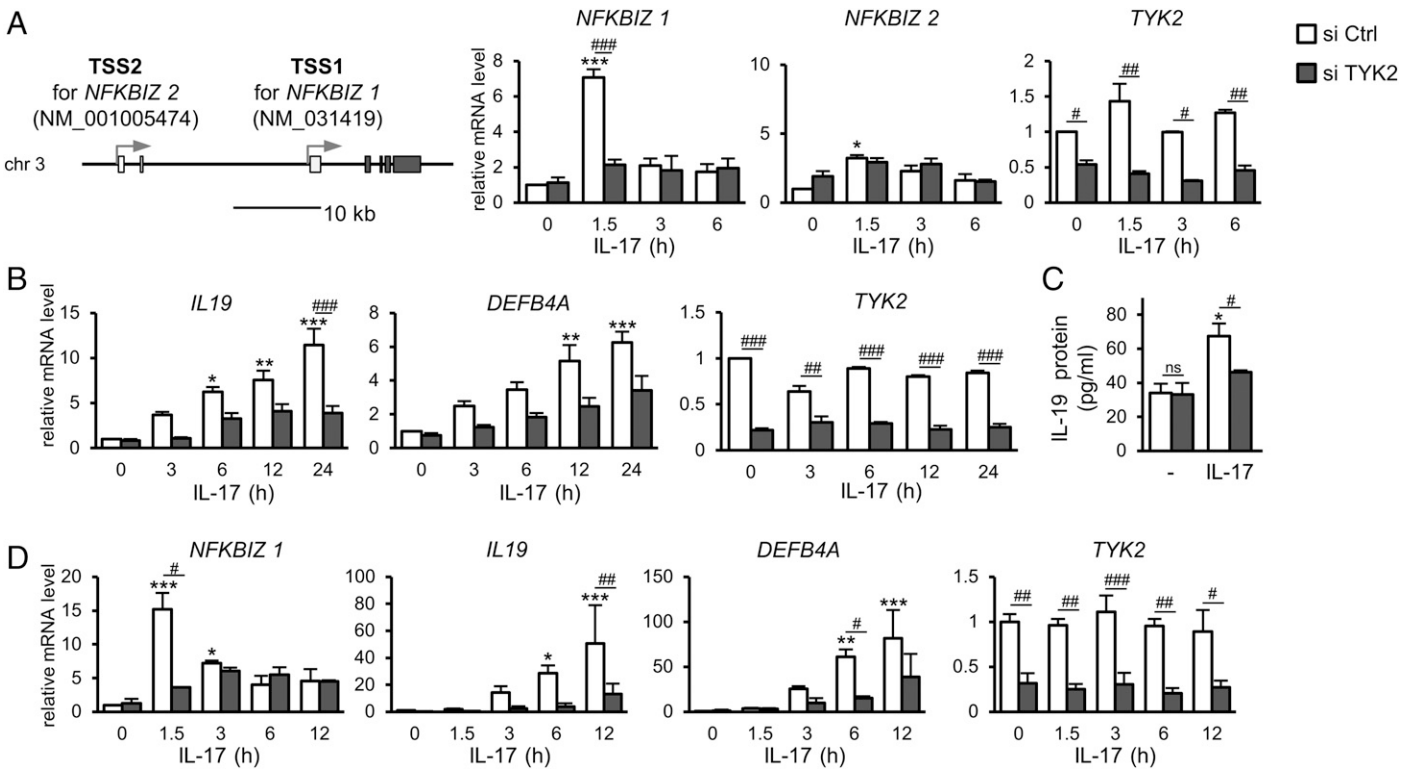

FIGURE 2. The effects of siRNA-mediated TYK2 knockdown on IL-17 response in keratinocytes.

(**A**) The induction of *NFKBIZ* transcriptional variant 1 was mediated by TYK2. HaCaT cells transfected with 20 pmol of TYK2 siRNA (siTYK2) or control siRNA (siCtrl) were stimulated with IL-17 (100 ng/ml) for the indicated times. The amount of *NFKBIZ* mRNA variant 1 or variant 2 was determined by qPCR. (**B**) Effects of TYK2 knockdown on the mRNA levels of IL-17–induced genes. HaCaT cells were treated as in (A) for the indicated times. The expression of indicated transcripts was measured and is shown as relative values. (**C**) The effect of TYK2 knockdown on IL-19 protein production. IL-19 protein levels in culture supernatants of cells treated as indicated for 24 h were analyzed by ELISA. (**D**) NHEKs were transfected with 20 pmol of siTYK2 or siCtrl. Twenty-four hours posttransfection, the cells were incubated with IL-17 (100 ng/ml) for the indicated times. The amount of *NFKBIZ 1* mRNA in HaCaT cells was determined by qPCR. Transcript expression is shown as relative values. Data are means of three independent experiments (±SEM). $^{*}p < 0.05$, $^{**}p < 0.01$, $^{***}p < 0.001$ compared with nontreated control; $^{\#}p < 0.05$, $^{\#\#}p < 0.01$, $^{\#\#\#}p < 0.001$ compared with siCtrl.

by CHX resulted in IκB-ζ mRNA accumulation in cells not treated with IL-17 (Fig. 4G). This CHX-induced accumulation of IκB-ζ mRNA was not significantly increased by combined stimulation with IL-17 (Fig. 4G). The treatment with transcription inhibitor actinomycin D completely abrogated CHX-induced accumulation of IκB-ζ mRNA in HaCaT cells (Fig. 4G), suggesting that CHX-induced accumulation of IκB-ζ mRNA is probably the reflection of the rate of IL-17–unrelated constitutive transcription of the IκB-ζ gene.

The TYK2–STAT3 pathway mediates IL-17–unrelated constitutive transcription of the IκB-ζ gene in HaCaT cells

We speculated that TYK2-mediated STAT3 activation may be required for constitutive transcription of IκB-ζ because STAT3 reportedly plays a critical role in maintaining epithelial cell survival via IκB-ζ induction (25). siRNA-mediated knockdown of STAT3 or TYK2 showed significant suppression of CHX-induced IκB-ζ accumulation (Fig. 5A). Western blot analysis showed that tyrosine phosphorylation of STAT3, which is a hallmark for STAT3 protein activation, constitutively occurs in HaCaT cells, and it was attenuated by TYK2 siRNA introduction (Fig. 5B). Treatment with IL-17 did not increase STAT3 phosphorylation levels (Fig. 5B), which seemed to be in accordance with data showing that IL-17 did not activate IκB-ζ promoter activity (Fig. 3B). ChIP experiments using the anti-STAT3 Ab showed that STAT3 constitutively binds to the genomic promoter region of IκB-ζ TSS1 in nontreated HaCaT cells (Fig. 5C). STAT3 did not show specific binding to the promoter region of IκB-ζ TSS2 (Fig. 5C), the induction of which was unrelated to TYK2 expression (Fig. 2A), suggesting that the constitutive transcription of IκB-ζ is mediated by the TYK2–STAT3 pathway in a promoter region–specific manner. The promoter region of IκB-ζ TSS1 contains two putative STAT-binding sites (Fig. 5D). The IκB-ζ-promoter-Luc responded to the plasmid overexpression of STAT3C, a constitutively active mutant of STAT3 (Fig. 5D). We mutated each of the putative STAT-binding sites in the IκB-ζ-promoter-Luc and performed luciferase assays to test the significance of STAT3 activity. As shown in Fig. 5D, the deletion of site 1 (−133 to −125) abolished the STAT3C-mediated promoter activation. In contrast, the deletion of site 2 (−462 to −453) did not affect the promoter activity. These results indicated that the TYK2–STAT3 pathway

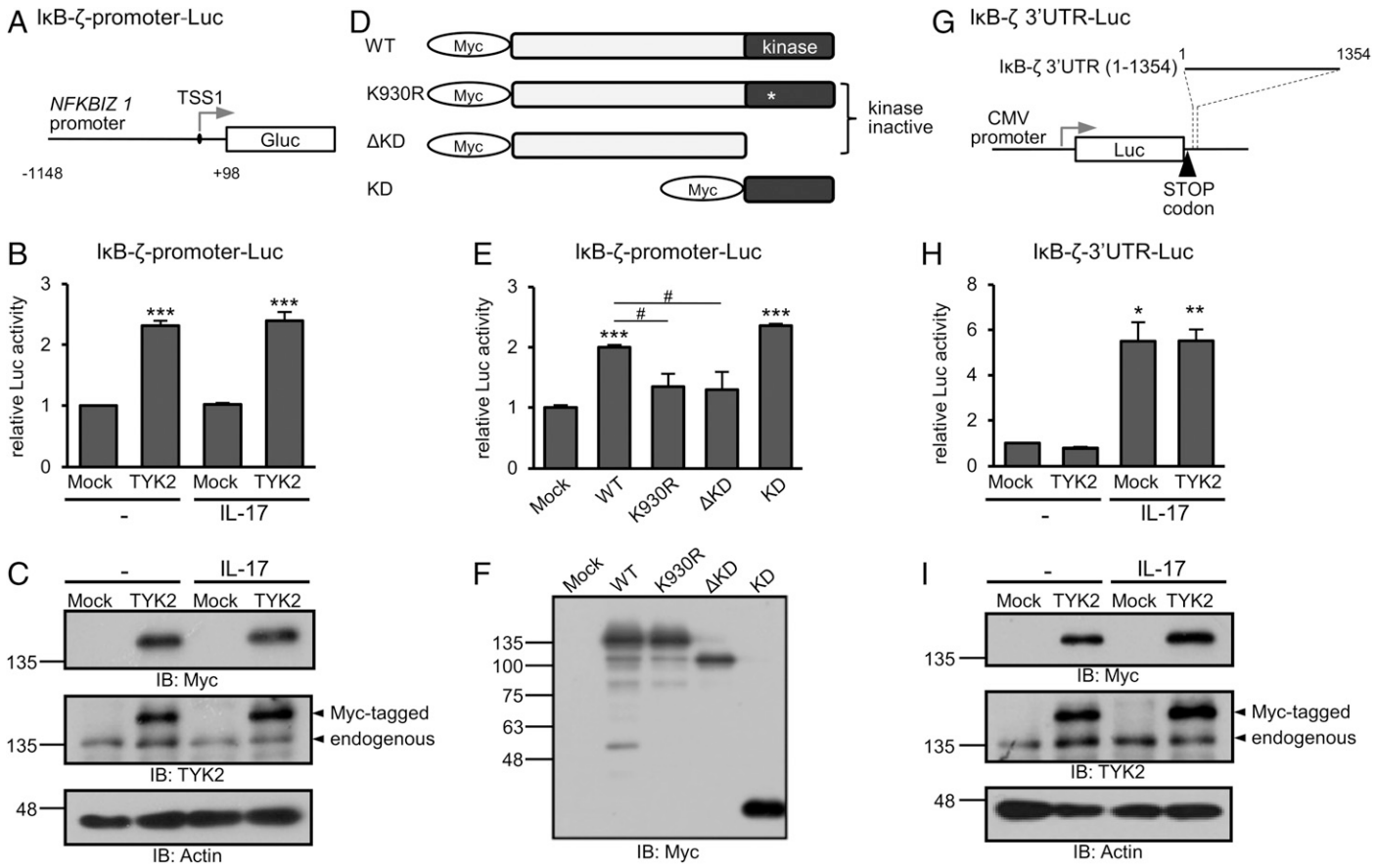

FIGURE 3. Distinct roles for TYK2 function and IL-17–induced signaling in IκB-ζ induction.

(**A**) Schematic representation of luciferase reporter construct ligated to the NFKBIZ1 promoter region (IκB-ζ-promoter-Luc). (**B**) Effects of TYK2 overexpression and/or IL-17 stimulation on IκB-ζ promoter activity. HeLa cells were transfected with the IκB-ζ-promoter-Luc construct with or without the plasmid expressing TYK2. At 36 h posttransfection, cells were treated with IL-17 (100 ng/ml) for an additional 1.5 h. The culture supernatants of the cells were collected and assayed for secreted Gluc activity. Data are representative of at least three independent experiments, each performed in triplicate, presented relative to the control (Mock-transfected cells), and shown as mean ± SEM. ***$p < 0.001$ compared with Mock-transfected control. (**C**) Total cell lysates from (B) were checked for TYK2 overexpression by Western blotting using anti–Myc-tag and anti-TYK2 Abs. Actin served as the loading control. (**D**) Schematic representation of TYK2 expression constructs. (**E**) HeLa cells were transfected with the IκB-ζ-promoter-Luc construct with each of the plasmids expressing TYK2 mutant or empty vector. At 36 h posttransfection, the culture supernatants of cells were collected and assayed for secreted Gluc activity. Data are representative of at least three independent experiments, each performed in triplicate, presented relative to Mock-transfected cells, and shown as mean ± SEM. ***$p < 0.001$ compared with Mock-transfected control; $^{\#}p < 0.05$ compared with TYK2 WT. (**F**) Total cell lysates from (E) were checked for overexpression of TYK2 constructs by Western blotting using anti–Myc-tag Ab. (**G**) Schematic representation of IκB-ζ 3′UTR-Luc. Full length of IκB-ζ 3′UTR was inserted immediately after the stop codon of the firefly luciferase coding sequence. (**H**) IL-17 stimulation stabilized IκB-ζ mRNA via its 3′UTR. HeLa cells were transfected with the IκB-ζ-3′UTR-Luc construct, together with the TYK2 expression plasmid or empty vector. At 36 h posttransfection, the cells were treated with IL-17 (100 ng/ml) for an additional 1.5 h. The cells were lysed and subjected to the reporter luciferase assay. Data are representative of at least three independent experiments, each performed in triplicate, presented relative to Mock-transfected cells, and shown as mean ± SEM. *$p < 0.05$, **$p < 0.01$ compared with Mock-transfected control. (**I**) Total cell lysates from (H) were checked for TYK2 overexpression by Western blotting.

drives IκB-ζ gene transcription with no particular requirement of IL-17 signaling.

JAK inhibitors suppress IL-17–induced expression of NFKBIZ

Similar to TYK2 knockdown (Fig. 2A), siRNA-mediated knockdown of STAT3 resulted in the suppression of IL-17–induced upregulation of IκB-ζ mRNA in HaCaT cells (Fig. 6A), suggesting that the transcription of IκB-ζ by STAT3 is required for IL-17–induced upregulation of IκB-ζ. However, IL-17 did not stimulate STAT3 phosphorylation (Fig. 5B). To further verify the significance of TYK2–STAT3 pathway in the induction of IκB-ζ, we pharmacologically inhibited STAT3 activity using three small-molecule JAK inhibitors (cerdulatinib, pyridone-6,

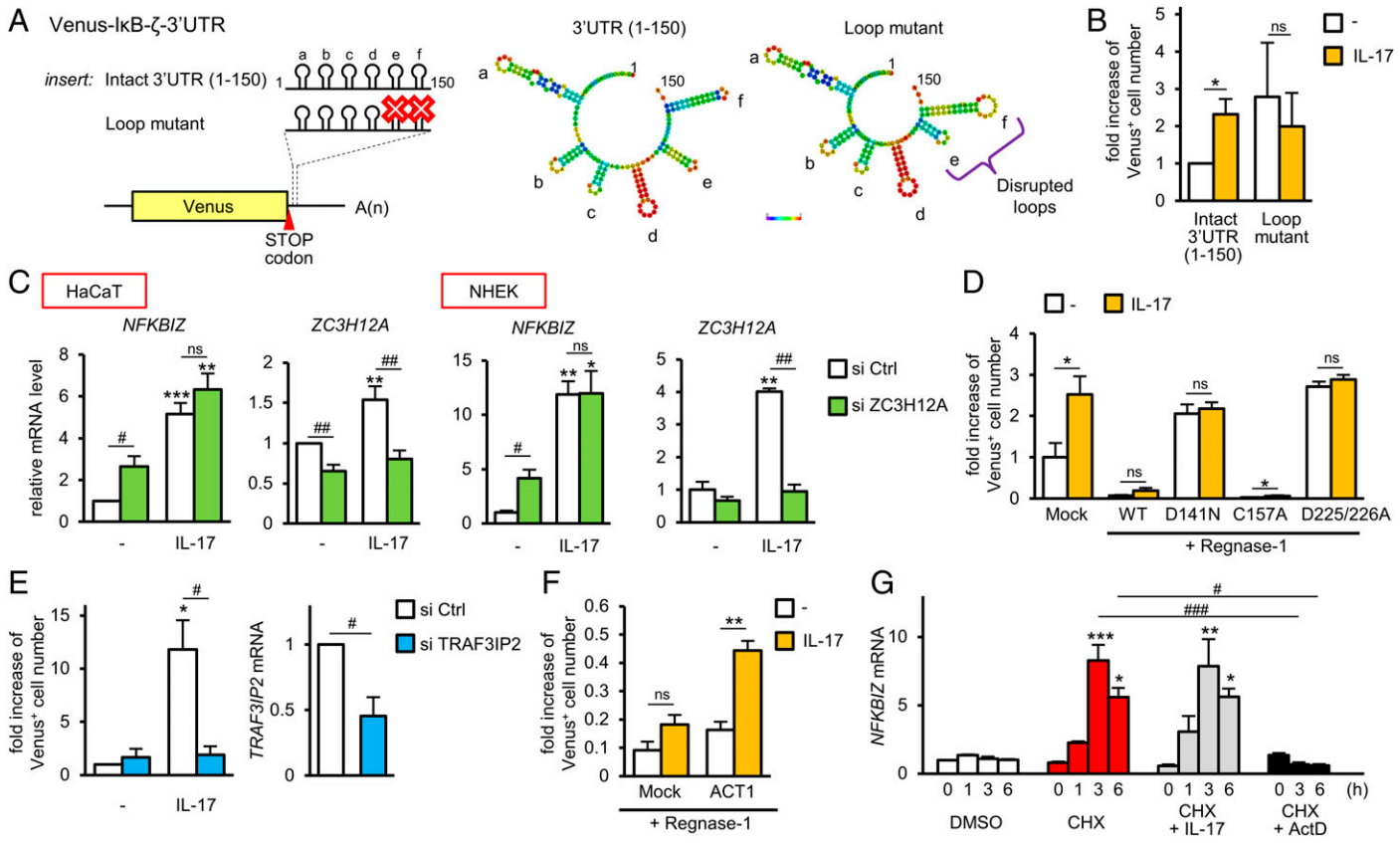

FIGURE 4. Regnase-1–mediated mRNA degradation was inhibited by IL-17 signaling.

(**A**) Left, Schematic representation of the Venus fluorescent reporter fused to the truncated portion (1–150) of the IκB-ζ-3′UTR. The loop mutant has mutations in sequences corresponding to two conserved stem-loops (indicated as "e" and "f"). Right, The secondary structures of the intact and mutated IκB-ζ-3′UTR mRNA (1–150) were predicted using the CentroidFold Web server (45) (http://www.ncrna.org). (**B**) The effect of loop disruption in the IκB-ζ-3′UTR on IL-17–induced posttranscriptional stabilization. HeLa cells were transfected with the Venus reporter fused to 1–150 nt of the IκB-ζ-3′UTR or its loop disruption mutant. The IL-17 (100 ng/ml)–induced change in numbers of Venus-positive cells was analyzed by flow cytometry. Data are mean ± SEM of three independent experiments and are presented as relative to unstimulated cells. $*p < 0.05$ compared with unstimulated cells. ns, not significant. (**C**) Constitutive suppression of endogenous IκB-ζ-mRNA by Regnase-1. HaCaT or NHEK cells transfected with 20 pmol of ZC3H12A-siRNA (siZC3H12A) or control siRNA (siCtrl) were stimulated with IL-17 (100 ng/ml) for 1.5 h. The amounts of IκB-ζ and ZC3H12A mRNA in cells were determined by qPCR. Transcript expression is shown as relative values. Data are mean ± SEM ($n = 4$). $*p < 0.05$, $**p < 0.01$, $*** p < 0.001$ compared with nontreated control; $^{\#}p < 0.05$, $^{\#\#}p < 0.01$ compared with siCtrl. (**D**) The effects of Regnase-1 overexpression on the Venus-IκB-ζ-3′UTR reporter. HeLa cells were transfected with the Venus-IκB-ζ-3′UTR reporter construct together with the expression vector for WT Regnase-1 or Regnase-1 mutants (D141N, C157A, and D225/226A). At 36 h posttransfection, the cells were left untreated or treated with IL-17 (100 ng/ml) for an additional 15 h. The number of Venus-positive cells was analyzed by flow cytometry. Data are representative of two independent experiments, each performed in triplicate, presented relative to Mock-transfected cells, and shown as mean ± SEM. $*p < 0.05$, compared with unstimulated control. ns, not significant. (**E**) HeLa cells were transfected with 20 pmol of TRAF3IP2 (ACT1) siRNA (siTRAF3IP2) or siCtrl. The cells were then transfected with the Venus-IκB-ζ-3′UTR reporter construct. Twenty-four hours posttransfection, the cells were incubated with or without IL-17 (100 ng/ml) for 15 h and were subjected to FACS analysis. The amounts of TRAF3IP2 mRNA in the cells at the time point of starting IL-17 treatment were determined by qPCR. Data are mean ± SEM ($n = 3$). $*p < 0.05$ compared with nontreated control; $^{\#}p < 0.05$ compared with siCtrl. (**F**) HeLa cells were transfected with the Venus-IκB-ζ-3′UTR reporter construct and Regnase-1 plasmid, together with the expression vector for ACT1 or empty vector. At 36 h posttransfection, the cells were left untreated or treated with IL-17 (100 ng/ml) for an additional 15 h and were subjected to FACS analysis. Data are representative of two independent experiments, each performed in triplicate, presented relative to Mock-transfected cells, and shown as mean ± SEM. $**p < 0.01$ compared with unstimulated control. ns, not significant. (**G**) Effect of translation inhibition on IκB-ζ mRNA levels. HaCaT cells were treated with DMSO, CHX (10 μg/ml), or CHX plus IL-17 (100 ng/ml) for indicated times. HaCaT cells pretreated with transcription inhibitor actinomycin D (ActD; 10 μg/ml) for 30 min were also treated with CHX as indicated. The amount of IκB-ζ mRNA was determined by qPCR. Transcript expression is shown as relative values. Data are mean ± SEM ($n = 4$). $*p < 0.05$, $**p < 0.01$, $***p < 0.001$ compared with nontreated control; $^{\#}p < 0.05$, $^{\#\#\#}p < 0.001$ compared with cells treated with CHX only.

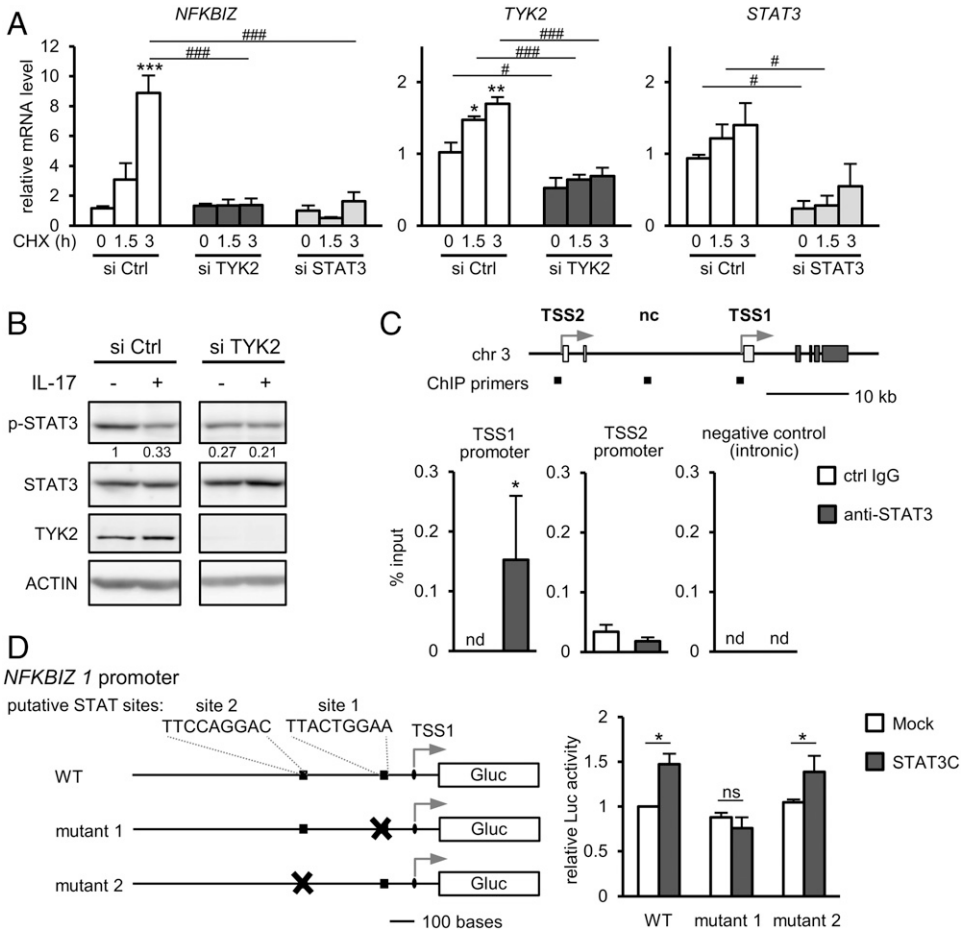

FIGURE 5. Transcription of IκB-ζ mRNA is constitutive and mediated by the TYK2–STAT3 pathway in HaCaT cells.

(**A**) The TYK2–STAT3 pathway mediates constitutive IκB-ζ mRNA transcription. HaCaT cells transfected with 20 pmol of TYK2 siRNA (siTYK2), STAT3 siRNA (siSTAT3), or control siRNA (siCtrl) were treated with CHX (10 μg/ml) for the indicated times. The amount of IκB-ζ mRNA in the cells was determined by qPCR. Transcript expression is shown as relative values. Data are mean ± SEM (n = 3). *$p < 0.05$, **$p < 0.01$, ***$p < 0.001$ compared with nontreated control; $^{\#}p < 0.05$, $^{\#\#\#}p < 0.001$ compared with siCtrl. (**B**) TYK2 maintains constitutive phosphorylation of STAT3 in HaCaT cells. HaCaT cells transfected with 20 pmol of siTYK2 or siCtrl were incubated with IL-17 (100 ng/ml) for 3 h. The cells were lysed and analyzed by Western blotting using indicated Abs. Densitometry values of phosphorylated STAT3 are expressed as fold change compared with control values normalized to 1. The experiment was repeated two times. (**C**) Constitutive binding of STAT3 to the promoter region of IκB-ζ variant 1. Nontreated HaCaT cells were lysed and subjected to ChIP assay using the anti-STAT3 Ab. STAT3-bound genomic DNA was PCR-amplified for different regions of IκB-ζ promoter as indicated. The means of percentage input values from three independent experiments are shown. Error bars represent SEM (n = 3). *$p < 0.01$ compared with normal IgG immunoprecipitation, which was the control. (**D**) Left, Schematic representation of intact TSS1 promoter with two putative STAT-binding sites and deletion mutants for each of the sites. Right, HeLa cells were transfected with each IκB-ζ-promoter-Luc construct, together with expression vector for the constitutively active form of STAT3 (STAT3C) as indicated. At 24 h posttransfection, the culture supernatants were collected, and luciferase activities were measured. Data are mean (±SEM) of three independent experiments and are presented relative to Mock-transfected cells. *$p < 0.05$ compared with Mock-transfected control. nd, not detected; ns, not significant.

and tofacitinib), each of which has been reported to have distinct JAK selectivity (52–54) (summarized in Fig. 6B). Cerdulatinib and pyridone-6, compared with tofacitinib, have relatively low IC_{50} values for TYK2 (52). IκB-ζ mRNA induction by IL-17 was suppressed by each of these three JAK inhibitors in a dose-dependent manner, with a relatively low effectiveness of tofacitinib (Fig. 6C). These JAK inhibitors efficiently suppressed the constitutive phosphorylation level of STAT3 (Fig. 6D). ChIP analysis showed that cerdulatinib addition abrogated constitutive STAT3 binding to the IκB-ζ TSS1 promoter region (Fig. 6E). Moreover, cerdulatinib treatment suppressed IL-17–induced increase of IκB-ζ and β-defensin 2 proteins (Fig. 6F). These results suggested that the activity of the TYK2–STAT3 pathway defines the strength of IL-17–induced expression of IκB-ζ in keratinocytes.

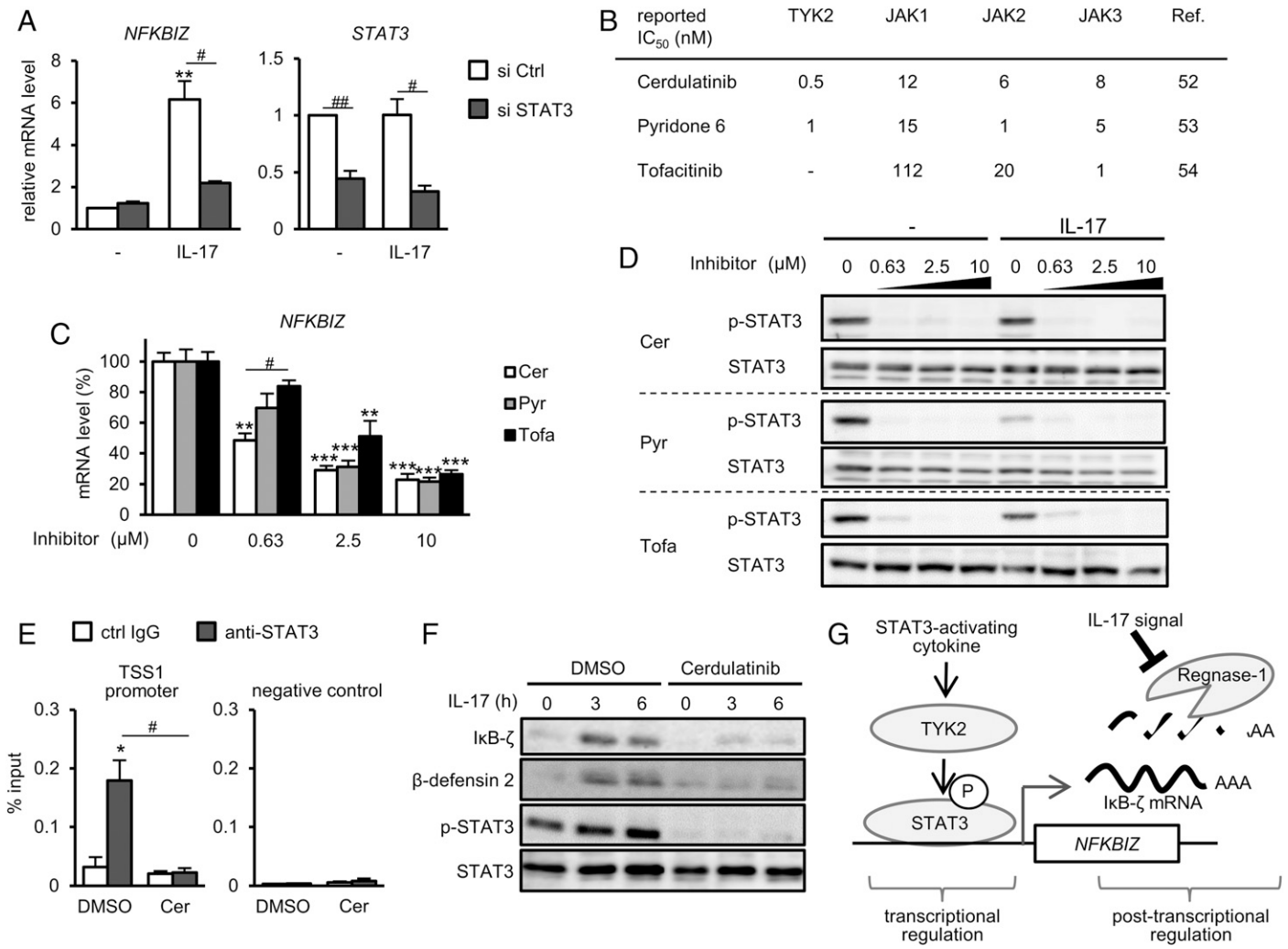

FIGURE 6. JAK inhibitors suppress IL-17–induced expression of IκB-ζ.

(**A**) HaCaT cells transfected with 20 pmol of STAT3 siRNA (siSTAT3) or control siRNA (siCtrl) were incubated with IL-17 (100 ng/ml) for 1.5 h. Transcript expression was analyzed by qPCR and shown as relative values. Data are mean ± SEM (n = 3). $^{**}p < 0.01$ compared with nontreated control; $^{\#}p < 0.05$, $^{\#\#}p < 0.01$ compared with siCtrl. (**B**) Summary of reported IC_{50} values of JAK inhibitors. (**C**) JAK inhibitors suppressed IL-17–induced IκB-ζ expression. HaCaT cells were pretreated with various concentrations of JAK inhibitors as indicated for 1 h and subsequently treated with IL-17 (100 ng/ml) for 1.5 h. The amount of IκB-ζ mRNA was determined by qPCR. Transcript expression is shown as relative values. Data are mean ± SEM (n = 3). $^{**}p < 0.01$, $^{***}p < 0.001$ compared with no inhibitor control; $^{\#}p < 0.05$ compared with cells treated with cerdulatinib. (**D**) JAK inhibitor treatment suppressed the level of constitutive STAT3 phosphorylation. Cell lysates were prepared from the cells treated as in (C) and analyzed by Western blotting analysis with an anti–phospho-STAT3 Ab. The experiment was repeated three times. (**E**) Cerdulatinib treatment compromised constitutive STAT3 binding to the IκB-ζ TSS1 promoter. HaCaT cells were treated with vehicle control or cerdulatinib (10 μM) for 1 h and subjected to ChIP with an anti-STAT3 Ab. The means of percentage input values from three independent experiments are shown. Error bars represent ±SEM. $^{*}p < 0.05$ compared with IgG immunoprecipitation (control); $^{\#}p < 0.05$ compared with DMSO treatment. (**F**) Cerdulatinib suppressed IL-17–induced upregulation of IκB-ζ and β-defensin 2 proteins. HaCaT cells were pretreated with cerdulatinib (0.63 μM) for 1 h and then stimulated with IL-17 (100 ng/ml) for 3 h. The cells were lysed and analyzed by Western blotting using indicated Abs. The experiment was repeated three times. (**G**) A model of IL-17–driven IκB-ζ expression in cells. STAT3 activity is required for the transcriptional activation of the IκB-ζ gene. IL-17–induced inactivation of Regnase-1 allows accumulation of IκB-ζ mRNA.

DISCUSSION

JAK/TYK2 inhibitors have been developed and intended to be used for psoriasis therapy (55–57). The basis of efficacy of TYK2 inhibition has been considered to be the suppression of lymphocyte activation, including IL-12/IFN-γ and IL-23/IL-17 axes (13, 18). In the current study, we investigated the role of TYK2 in IL-17 responsiveness in epithelial (nonlymphocyte) cells and

https://doi.org/10.4049/immunohorizons.1900023

demonstrated that TYK2-mediated maintenance of STAT3 phosphorylation is a substantial driver for the keratinocyte IL-17 response via IκB-ζ gene transcription. This finding expands our understanding of the mechanism of action of clinically used TYK2 selective inhibitors. We speculated that TYK2 inhibition can suppress IL-17–induced keratinocyte activation in addition to IL-12/IFN-γ and IL-23/IL-17 axes, thus showing high clinical efficacy.

The transcription factor STAT3 is a well-known kinase substrate of JAK/TYK2 and has a major function in the signal transduction of psoriatic keratinocytes in response to cytokine/growth factors (23, 58–61). In the current study, we showed that the TYK2-mediated STAT3 phosphorylation is a rate determinant for the IL-17–unrelated transcription of the IκB-ζ gene and that pharmacological inhibitors of JAKs could be used to suppress the transcription. In psoriatic lesions, the persistently enhanced phosphorylation of STAT3 in keratinocytes occurs more as the effects of various cytokines become pronounced, such as IL-19, IL-21, IL-22, IL-25, and IL-36, which are upregulated in lesions (23, 60, 61). As a result, enhanced transcription of the IκB-ζ gene by STAT3 occurs, and this STAT3 action is the therapeutic target of JAK/TYK2 inhibitors. Our previous study (14) demonstrated that TYK2-deficient mice possessed diminished skin inflammation and psoriasis-like pathologic condition after direct IL-22 injection into ear pinna. We showed that TYK2 plays a role in STAT3 phosphorylation in IL-22–treated keratinocytes. These previous observations supported the idea that TYK2 is required not only for T cell–dependent inflammation but also for non–T cell reactions in a dermatitis pathologic condition, such as keratinocyte activation. The promoter activation effect by WT TYK2 overexpression was only ~2-fold in HeLa cells (Fig. 3B). We speculate that background STAT3 activity had an effect to worsen the experimentally observed signal/noise ratio in the reporter system that is transcriptionally activated by STAT3. Indeed, in HeLa (data not shown) and HaCaT (Fig. 5B) cells, phosphorylated STAT3 is constantly detected even without introducing exogenous TYK2. Nevertheless, the result that overexpression of WT but not kinase-inactive mutant TYK2 enhanced IκB-ζ promoter activity (Fig. 3E) supported the contribution of catalytic activity of TYK2.

We demonstrated that the TYK2–STAT3 pathway regulated promoter-selective induction of human IκB-ζ. Publicly available genome and transcripts data (Gene identification number 64332 for human IκB-ζ and 80859 for mouse) in the National Center for Biotechnology Information Gene database (https://www.ncbi.nlm.nih.gov/gene/) show that the overall gene structure, as well as the two major TSS (described as TSS1 and TSS2 in the present paper), are conserved between human and mouse IκB-ζ genes (Supplemental Fig. 1). The promoter activity for upstream-located TSS2 has been investigated and revealed to be regulated by NF-κB transcription factor (24). However, the transcriptional regulatory mechanism at the downstream-located TSS1 was unclear. In the current study, we demonstrated the role of STAT3 in the transcription from TSS1. We identified site 1 (5′-TTACTGGAA-3′) at the position upstream (−133 to −125) of TSS1 as a STAT-binding sequence (Fig. 5D). Comparative genomic analysis showed that site 1 is well conserved among multiple mammalian species (Supplemental Fig. 2), suggesting the importance of this STAT-binding site for IκB-ζ gene transcription. A recent study using RNA sequencing analysis of IL-36–stimulated keratinocytes has provided a clear example that the downstream-located promoter region (corresponding to TSS1 in the present paper) is the dominant promoter used for IκB-ζ transcription in keratinocytes (23). Also, in that study, STAT3 involvement in the TSS1 promoter regulation has been shown. Our data are consistent with these previous results and, thus, reasonably support the possibility of the use of JAK/TYK2 inhibitors for targeting keratinocytes.

It should be noted that no difference in *Nfkbiz* mRNA levels was found between WT and TYK2 knockout (KO) under the conditions without IMQ application (Fig. 1B). Also, TYK2 knockdown in HaCaT cells did not decrease *NFKBIZ* mRNA under nonstimulated conditions (Fig. 2A). These results implied that IκB-ζ mRNA levels were determined not solely by the activity of the TYK2–STAT3 pathway and that without IL-17, the effects of TYK2 knockdown on IκB-ζ mRNA levels do not emerge. Thus, a specific IL-17–elicited event may be required for efficient IκB-ζ induction. In the current study, we focused on Regnase-1–mediated posttranscriptional stability control of mRNA. Constitutive activity of endogenous Regnase-1 appeared to play a more important role than the TYK2–STAT3 pathway in terms of determining the basal expression level of IκB-ζ (Fig. 4C). In addition, our results showed that IL-17 signaling seemed to act as the key for the deactivation of posttranscriptional mRNA degradation mediated by Regnase-1. The transient inhibition of Regnase-1 in IL-17–treated keratinocytes can be achieved promptly through proteasome-mediated degradation, as reported recently (33). This brake-releasing mechanism may allow for the accumulation of IL-17–induced mRNA. TYK2–STAT3–mediated transcription is considered to have a substantial (visible) role in driving IκB-ζ expression, especially when combined with the stimulation that suppresses Regnase-1 activity, such as IL-17 (Fig. 2) and CHX (Fig. 5A). Altogether, the combined activation of STAT3 and IL-17 signaling is important to elicit successful expression of the IκB-ζ protein (Fig. 6G).

To inhibit posttranscriptional mRNA destabilization and experimentally monitor the rate of IL-17–unrelated constitutive transcription of the IκB-ζ gene, we used protein translation inhibitor CHX. CHX has been shown to block Regnase-1–mediated destabilization of target mRNAs, the mechanism of which is translation-coupled (39). In the current study, we showed that CHX treatment can actually accumulate IκB-ζ mRNA in HaCaT cells (Fig. 4G), supporting the idea that Regnase-1 constitutively degrades IκB-ζ mRNA. The mRNA stabilizing effect of CHX is consistent with results from earlier studies that have shown that CHX treatment increases IκB-ζ and CXCL8 mRNA (62, 63), both of which have been reported to be degraded by Regnase-1 (39, 64). We showed that CHX-induced accumulation of IκB-ζ mRNA was not enhanced by combined stimulation with IL-17 (Fig. 4G). These observations supported the idea that the pathway targeted by IL-17 signaling may correspond to Regnase-1 activity.

The persistently high expression of IκB-ζ is considered to be pathogenic and can be a candidate therapeutic target in psoriasis (19). In addition, the complete absence of the IκB-ζ protein in murine epithelial cells exhibited elevated apoptosis, which triggers lymphocyte-mediated autoimmune inflammation resembling Sjögren syndrome (25), suggesting the indispensable function of epithelial IκB-ζ in the maintenance of cell viability and immune homeostasis. These findings indicated that IκB-ζ protein levels should be under tight regulation at an adequate level and should avoid persistent aberrant upregulation. Regnase-1 has been shown as an IL-17–inducible protein and a negative feedback inhibitor of IL-17–induced inflammation (31); it would be reasonable to consider that this feedback mechanism accounts for the prevention of persistent upregulation of the IκB-ζ protein. However, the mechanisms of constitutively regulated expression and IL-17–induced rapid induction of IκB-ζ were elusive. In the current study, we demonstrated that the regulated balance between the supply of IκB-ζ mRNA by STAT3 activity and constitutive degradation of IκB-ζ mRNA by Regnase-1 determines the steady-state expression level of IκB-ζ. It should be emphasized that Regnase-1 seems to suppress IκB-ζ expression not just as an IL-17–inducible negative feedback inhibitor but as a constitutive inhibitor. We speculated that IL-17–induced rapid IκB-ζ upregulation is attributed to the STAT3-driven transcription of IκB-ζ mRNA, which presumably omits the latency time required for multiple processes, including signal transduction, transcription factor activation, and mRNA synthesis. Overall, this regulatory system might enable cells both to express IκB-ζ protein at a level pertinent for cell viability and to quickly exert boosted induction if there is a need to fight against extrinsic fungal and bacterial infections.

In summary, we demonstrated that TYK2-mediated phosphorylation of STAT3 underlies the transcription of IκB-ζ. This IL-17–independent supply of IκB-ζ mRNA may act as a determinant for the strength of IL-17–induced responses in keratinocytes. This finding suggested that JAK/TYK2 inhibition can bring simultaneous inhibition of the IL-12/IL-23 responses in lymphocytes and the IL-17 response in keratinocytes of psoriatic lesions. Thus, JAK/TYK2 inhibition may be an effective method to treat IL-17–mediated diseases.

DISCLOSURES

The authors have no financial conflicts of interest.

ACKNOWLEDGMENTS

We express our gratitude to Dr. James N. Ihle (St. Jude Children's Research Hospital, Memphis, TN), Dr. Osamu Takeuchi (Kyoto University, Kyoto, Japan), Dr. Connie Cepko (Harvard Medical School, Boston, MA), and Dr. Steven Vogel (National Institutes of Health, Rockville, MD) for providing plasmids. We gratefully acknowledge the generous support of the Hokkaido University Global Facility Center Pharma Science Open Unit, which is funded by the Ministry of Education, Culture, Sports, Science and Technology–Japan under the Support Program for Implementation of New Equipment Sharing System.

REFERENCES

1. Nestle, F. O., D. H. Kaplan, and J. Barker. 2009. Psoriasis. *N. Engl. J. Med.* 361: 496–509.
2. Lowes, M. A., M. Suárez-Fariñas, and J. G. Krueger. 2014. Immunology of psoriasis. *Annu. Rev. Immunol.* 32: 227–255.
3. Lynde, C. W., Y. Poulin, R. Vender, M. Bourcier, and S. Khalil. 2014. Interleukin 17A: toward a new understanding of psoriasis pathogenesis. *J. Am. Acad. Dermatol.* 71: 141–150.
4. Baliwag, J., D. H. Barnes, and A. Johnston. 2015. Cytokines in psoriasis. *Cytokine* 73: 342–350.
5. Nograles, K. E., L. C. Zaba, E. Guttman-Yassky, J. Fuentes-Duculan, M. Suárez-Fariñas, I. Cardinale, A. Khatcherian, J. Gonzalez, K. C. Pierson, T. R. White, et al. 2008. Th17 cytokines interleukin (IL)-17 and IL-22 modulate distinct inflammatory and keratinocyte-response pathways. *Br. J. Dermatol.* 159: 1092–1102.
6. Chiricozzi, A., E. Guttman-Yassky, M. Suárez-Fariñas, K. E. Nograles, S. Tian, I. Cardinale, S. Chimenti, and J. G. Krueger. 2011. Integrative responses to IL-17 and TNF-α in human keratinocytes account for key inflammatory pathogenic circuits in psoriasis. *J. Invest. Dermatol.* 131: 677–687.
7. Xu, S., and X. Cao. 2010. Interleukin-17 and its expanding biological functions. *Cell. Mol. Immunol.* 7: 164–174.
8. Albanesi, C., S. Madonna, P. Gisondi, and G. Girolomoni. 2018. The interplay between keratinocytes and immune cells in the pathogenesis of psoriasis. *Front. Immunol.* 9: 1549.
9. Mease, P. J. 2015. Inhibition of interleukin-17, interleukin-23 and the TH17 cell pathway in the treatment of psoriatic arthritis and psoriasis. *Curr. Opin. Rheumatol.* 27: 127–133.
10. Shimoda, K., K. Kato, K. Aoki, T. Matsuda, A. Miyamoto, M. Shibamori, M. Yamashita, A. Numata, K. Takase, S. Kobayashi, et al. 2000. Tyk2 plays a restricted role in IFN alpha signaling, although it is required for IL-12-mediated T cell function. *Immunity* 13: 561–571.
11. Karaghiosoff, M., H. Neubauer, C. Lassnig, P. Kovarik, H. Schindler, H. Pircher, B. McCoy, C. Bogdan, T. Decker, G. Brem, et al. 2000. Partial impairment of cytokine responses in Tyk2-deficient mice. *Immunity* 13: 549–560.
12. Parham, C., M. Chirica, J. Timans, E. Vaisberg, M. Travis, J. Cheung, S. Pflanz, R. Zhang, K. P. Singh, F. Vega, et al. 2002. A receptor for the heterodimeric cytokine IL-23 is composed of IL-12Rbeta1 and a novel cytokine receptor subunit, IL-23R. *J. Immunol.* 168: 5699–5708.
13. Ishizaki, M., T. Akimoto, R. Muromoto, M. Yokoyama, Y. Ohshiro, Y. Sekine, H. Maeda, K. Shimoda, K. Oritani, and T. Matsuda. 2011. Involvement of tyrosine kinase-2 in both the IL-12/Th1 and IL-23/Th17 axes in vivo. *J. Immunol.* 187: 181–189.
14. Ishizaki, M., R. Muromoto, T. Akimoto, Y. Sekine, S. Kon, M. Diwan, H. Maeda, S. Togi, K. Shimoda, K. Oritani, and T. Matsuda. 2014. Tyk2 is a therapeutic target for psoriasis-like skin inflammation. *Int. Immunol.* 26: 257–267.
15. Strange, A., F. Capon, C. C. Spencer, J. Knight, M. E. Weale, M. H. Allen, A. Barton, G. Band, C. Bellenguez, J. G. Bergboer, et al; Genetic Analysis of Psoriasis Consortium & the Wellcome Trust Case Control Consortium 2. 2010. A genome-wide association study identifies new psoriasis susceptibility loci and an interaction between HLA-C and ERAP1. *Nat. Genet.* 42: 985–990.
16. Ellinghaus, D., E. Ellinghaus, R. P. Nair, P. E. Stuart, T. Esko, A. Metspalu, S. Debrus, J. V. Raelson, T. Tejasvi, M. Belouchi, et al. 2012. Combined analysis of genome-wide association studies for Crohn disease and psoriasis identifies seven shared susceptibility loci. *Am. J. Hum. Genet.* 90: 636–647.

17. Tsoi, L. C., S. L. Spain, E. Ellinghaus, P. E. Stuart, F. Capon, J. Knight, T. Tejasvi, H. M. Kang, M. H. Allen, S. Lambert, et al. 2015. Enhanced meta-analysis and replication studies identify five new psoriasis susceptibility loci. *Nat. Commun.* 6: 7001.
18. Works, M. G., F. Yin, C. C. Yin, Y. Yiu, K. Shew, T. T. Tran, N. Dunlap, J. Lam, T. Mitchell, J. Reader, et al. 2014. Inhibition of TYK2 and JAK1 ameliorates imiquimod-induced psoriasis-like dermatitis by inhibiting IL-22 and the IL-23/IL-17 axis. *J. Immunol.* 193: 3278–3287.
19. Johansen, C., M. Mose, P. Ommen, T. Bertelsen, H. Vinter, S. Hailfinger, S. Lorscheid, K. Schulze-Osthoff, and L. Iversen. 2015. IκBζ is a key driver in the development of psoriasis. *Proc. Natl. Acad. Sci. USA* 112: E5825–E5833.
20. Muromoto, R., T. Hirao, K. Tawa, K. Hirashima, S. Kon, Y. Kitai, and T. Matsuda. 2016. IL-17A plays a central role in the expression of psoriasis signature genes through the induction of IκB-ζ in keratinocytes. *Int. Immunol.* 28: 443–452.
21. Willems, M., N. Dubois, L. Musumeci, V. Bours, and P. A. Robe. 2016. IκBζ: an emerging player in cancer. *Oncotarget* 7: 66310–66322.
22. Bertelsen, T., C. Ljungberg, R. Boye Kjellerup, L. Iversen, and C. Johansen. 2017. IL-17F regulates psoriasis-associated genes through IκBζ. *Exp. Dermatol.* 26: 234–241.
23. Müller, A., A. Hennig, S. Lorscheid, P. Grondona, K. Schulze-Osthoff, S. Hailfinger, and D. Kramer. 2018. IκBζ is a key transcriptional regulator of IL-36-driven psoriasis-related gene expression in keratinocytes. *Proc. Natl. Acad. Sci. USA* 115: 10088–10093.
24. Yamazaki, S., T. Muta, S. Matsuo, and K. Takeshige. 2005. Stimulus-specific induction of a novel nuclear factor-kappaB regulator, IkappaB-zeta, via toll/interleukin-1 receptor is mediated by mRNA stabilization. *J. Biol. Chem.* 280: 1678–1687.
25. Okuma, A., K. Hoshino, T. Ohba, S. Fukushi, S. Aiba, S. Akira, M. Ono, T. Kaisho, and T. Muta. 2013. Enhanced apoptosis by disruption of the STAT3-IκB-ζ signaling pathway in epithelial cells induces Sjögren's syndrome-like autoimmune disease. *Immunity* 38: 450–460.
26. Amatya, N., A. V. Garg, and S. L. Gaffen. 2017. IL-17 signaling: the yin and the yang. *Trends Immunol.* 38: 310–322.
27. Hartupee, J., C. Liu, M. Novotny, X. Li, and T. Hamilton. 2007. IL-17 enhances chemokine gene expression through mRNA stabilization. *J. Immunol.* 179: 4135–4141.
28. Herjan, T., L. Hong, J. Bubenik, K. Bulek, W. Qian, C. Liu, X. Li, X. Chen, H. Yang, S. Ouyang, et al. 2018. IL-17–receptor-associated adaptor Act1 directly stabilizes mRNAs to mediate IL-17 inflammatory signaling. *Nat. Immunol.* 19: 354–365.
29. Amatya, N., E. E. Childs, J. A. Cruz, F. E. Y. Aggor, A. V. Garg, A. J. Berman, J. E. Gudjonsson, U. Atasoy, and S. L. Gaffen. 2018. IL-17 integrates multiple self-reinforcing, feed-forward mechanisms through the RNA binding protein Arid5a. *Sci. Signal.* 11: eaat4617.
30. Dhamija, S., R. Winzen, A. Doerrie, G. Behrens, N. Kuehne, C. Schauerte, E. Neumann, O. Dittrich-Breiholz, M. Kracht, and H. Holtmann. 2013. Interleukin-17 (IL-17) and IL-1 activate translation of overlapping sets of mRNAs, including that of the negative regulator of inflammation, MCPIP1. *J. Biol. Chem.* 288: 19250–19259.
31. Garg, A. V., N. Amatya, K. Chen, J. A. Cruz, P. Grover, N. Whibley, H. R. Conti, G. Hernandez Mir, T. Sirakova, E. C. Childs, et al. 2015. MCPIP1 endoribonuclease activity negatively regulates interleukin-17-mediated signaling and inflammation. *Immunity* 43: 475–487.
32. Monin, L., J. E. Gudjonsson, E. E. Childs, N. Amatya, X. Xing, A. H. Verma, B. M. Coleman, A. V. Garg, M. Killeen, A. Mathers, et al. 2017. MCPIP1/regnase-1 restricts IL-17A- and IL-17C-dependent skin inflammation. *J. Immunol.* 198: 767–775.
33. Takaishi, M., T. Satoh, S. Akira, and S. Sano. 2018. Regnase-1, an immunomodulator, limits the IL-36/IL-36R autostimulatory loop in keratinocytes to suppress skin inflammation. *J. Invest. Dermatol.* 138: 1439–1442.
34. Ruiz-Romeu, E., M. Ferran, A. Giménez-Arnau, B. Bugara, B. Lipert, J. Jura, E. F. Florencia, E. P. Prens, A. Celada, R. M. Pujol, and L. F. Santamaria-Babí. 2016. MCPIP1 RNase is aberrantly distributed in psoriatic epidermis and rapidly induced by IL-17A. *J. Invest. Dermatol.* 136: 1599–1607.
35. Matsushita, K., O. Takeuchi, D. M. Standley, Y. Kumagai, T. Kawagoe, T. Miyake, T. Satoh, H. Kato, T. Tsujimura, H. Nakamura, and S. Akira. 2009. Zc3h12a is an RNase essential for controlling immune responses by regulating mRNA decay. *Nature* 458: 1185–1190.
36. Iwasaki, H., O. Takeuchi, S. Teraguchi, K. Matsushita, T. Uehata, K. Kuniyoshi, T. Satoh, T. Saitoh, M. Matsushita, D. M. Standley, and S. Akira. 2011. The IκB kinase complex regulates the stability of cytokine-encoding mRNA induced by TLR-IL-1R by controlling degradation of regnase-1. *Nat. Immunol.* 12: 1167–1175.
37. Uehata, T., H. Iwasaki, A. Vandenbon, K. Matsushita, E. Hernandez-Cuellar, K. Kuniyoshi, T. Satoh, T. Mino, Y. Suzuki, D. M. Standley, et al. 2013. Malt1-induced cleavage of regnase-1 in CD4(+) helper T cells regulates immune activation. *Cell* 153: 1036–1049.
38. Jeltsch, K. M., D. Hu, S. Brenner, J. Zöller, G. A. Heinz, D. Nagel, K. U. Vogel, N. Rehage, S. C. Warth, S. L. Edelmann, et al. 2014. Cleavage of roquin and regnase-1 by the paracaspase MALT1 releases their cooperatively repressed targets to promote T(H)17 differentiation. *Nat. Immunol.* 15: 1079–1089.
39. Mino, T., Y. Murakawa, A. Fukao, A. Vandenbon, H. H. Wessels, D. Ori, T. Uehata, S. Tartey, S. Akira, Y. Suzuki, et al. 2015. Regnase-1 and roquin regulate a common element in inflammatory mRNAs by spatiotemporally distinct mechanisms. *Cell* 161: 1058–1073.
40. Behrens, G., R. Winzen, N. Rehage, A. Dörrie, M. Barsch, A. Hoffmann, J. Hackermüller, C. Tiedje, V. Heissmeyer, and H. Holtmann. 2018. A translational silencing function of MCPIP1/Regnase-1 specified by the target site context. *Nucleic Acids Res.* 46: 4256–4270.
41. Muromoto, R., M. Nakajima, K. Hirashima, T. Hirao, S. Kon, K. Shimoda, K. Oritani, and T. Matsuda. 2013. Jun activation domain-binding protein 1 (JAB1) is required for the optimal response to interferons. *J. Biol. Chem.* 288: 30969–30979.
42. Togi, S., R. Muromoto, K. Hirashima, Y. Kitai, T. Okayama, O. Ikeda, N. Matsumoto, S. Kon, Y. Sekine, K. Oritani, and T. Matsuda. 2016. A new STAT3-binding partner, ARL3, enhances the phosphorylation and nuclear accumulation of STAT3. *J. Biol. Chem.* 291: 11161–11171.
43. Matsuda, T., and C. L. Cepko. 2004. Electroporation and RNA interference in the rodent retina in vivo and in vitro. *Proc. Natl. Acad. Sci. USA* 101: 16–22.
44. Koushik, S. V., H. Chen, C. Thaler, H. L. Puhl III, and S. S. Vogel. 2006. Cerulean, venus, and venusY67C FRET reference standards. *Biophys. J.* 91: L99–L101.
45. Sato, K., M. Hamada, K. Asai, and T. Mituyama. 2009. CENTROIDFOLD: a web server for RNA secondary structure prediction. *Nucleic Acids Res.* 37(Suppl. 2): W277–W280.
46. Muromoto, R., M. Ishida, K. Sugiyama, Y. Sekine, K. Oritani, K. Shimoda, and T. Matsuda. 2006. Sumoylation of Daxx regulates IFN-induced growth suppression of B lymphocytes and the hormone receptor-mediated transactivation. *J. Immunol.* 177: 1160–1170.
47. Muromoto, R., M. Kuroda, S. Togi, Y. Sekine, A. Nanbo, K. Shimoda, K. Oritani, and T. Matsuda. 2010. Functional involvement of Daxx in gp130-mediated cell growth and survival in BaF3 cells. *Eur. J. Immunol.* 40: 3570–3580.
48. Johansen, C., P. A. Usher, R. B. Kjellerup, D. Lundsgaard, L. Iversen, and K. Kragballe. 2009. Characterization of the interleukin-17 isoforms and receptors in lesional psoriatic skin. *Br. J. Dermatol.* 160: 319–324.
49. van der Fits, L., S. Mourits, J. S. Voerman, M. Kant, L. Boon, J. D. Laman, F. Cornelissen, A. M. Mus, E. Florencia, E. P. Prens, and E. Lubberts. 2009. Imiquimod-induced psoriasis-like skin inflammation in mice is mediated via the IL-23/IL-17 axis. *J. Immunol.* 182: 5836–5845.
50. Qi, D., S. Huang, R. Miao, Z. G. She, T. Quinn, Y. Chang, J. Liu, D. Fan, Y. E. Chen, and M. Fu. 2011. Monocyte chemotactic protein-induced

protein 1 (MCPIP1) suppresses stress granule formation and determines apoptosis under stress. *J. Biol. Chem.* 286: 41692–41700.
51. Qian, Y., C. Liu, J. Hartupee, C. Z. Altuntas, M. F. Gulen, D. Jane-Wit, J. Xiao, Y. Lu, N. Giltiay, J. Liu, et al. 2007. The adaptor Act1 is required for interleukin 17-dependent signaling associated with autoimmune and inflammatory disease. *Nat. Immunol.* 8: 247–256.
52. Coffey, G., A. Betz, F. DeGuzman, Y. Pak, M. Inagaki, D. C. Baker, S. J. Hollenbach, A. Pandey, and U. Sinha. 2014. The novel kinase inhibitor PRT062070 (Cerdulatinib) demonstrates efficacy in models of autoimmunity and B-cell cancer. *J. Pharmacol. Exp. Ther.* 351: 538–548.
53. Thompson, J. E., R. M. Cubbon, R. T. Cummings, L. S. Wicker, R. Frankshun, B. R. Cunningham, P. M. Cameron, P. T. Meinke, N. Liverton, Y. Weng, and J. A. DeMartino. 2002. Photochemical preparation of a pyridone containing tetracycle: a Jak protein kinase inhibitor. *Bioorg. Med. Chem. Lett.* 12: 1219–1223.
54. Jiang, J. K., K. Ghoreschi, F. Deflorian, Z. Chen, M. Perreira, M. Pesu, J. Smith, D. T. Nguyen, E. H. Liu, W. Leister, et al. 2008. Examining the chirality, conformation and selective kinase inhibition of 3-((3R,4R)-4-methyl-3-(methyl(7H-pyrrolo[2,3-d]pyrimidin-4-yl)amino) piperidin-1-yl)-3-oxopropanenitrile (CP-690,550). *J. Med. Chem.* 51: 8012–8018.
55. Papp, K., K. Gordon, D. Thaçi, A. Morita, M. Gooderham, P. Foley, I. G. Girgis, S. Kundu, and S. Banerjee. 2018. Phase 2 trial of selective tyrosine kinase 2 inhibition in psoriasis. *N. Engl. J. Med.* 379: 1313–1321.
56. Banfield, C., M. Scaramozza, W. Zhang, E. Kieras, K. M. Page, A. Fensome, M. Vincent, M. E. Dowty, K. Goteti, P. J. Winkle, and E. Peeva. 2018. The safety, tolerability, pharmacokinetics, and pharmacodynamics of a TYK2/JAK1 inhibitor (PF-06700841) in healthy subjects and patients with plaque psoriasis. *J. Clin. Pharmacol.* 58: 434–447.
57. Bachelez, H., P. C. van de Kerkhof, R. Strohal, A. Kubanov, F. Valenzuela, J. H. Lee, V. Yakusevich, S. Chimenti, J. Papacharalambous, J. Proulx, et al; OPT Compare Investigators. 2015. Tofacitinib versus etanercept or placebo in moderate-to-severe chronic plaque psoriasis: a phase 3 randomised non-inferiority trial. *Lancet* 386: 552–561.
58. Sano, S., K. S. Chan, S. Carbajal, J. Clifford, M. Peavey, K. Kiguchi, S. Itami, B. J. Nickoloff, and J. DiGiovanni. 2005. Stat3 links activated keratinocytes and immunocytes required for development of psoriasis in a novel transgenic mouse model. *Nat. Med.* 11: 43–49.
59. Miyoshi, K., M. Takaishi, K. Nakajima, M. Ikeda, T. Kanda, M. Tarutani, T. Iiyama, N. Asao, J. DiGiovanni, and S. Sano. 2011. Stat3 as a therapeutic target for the treatment of psoriasis: a clinical feasibility study with STA-21, a Stat3 inhibitor. *J. Invest. Dermatol.* 131: 108–117.
60. Calautti, E., L. Avalle, and V. Poli. 2018. Psoriasis: a STAT3-centric view. *Int. J. Mol. Sci.* 19: 171.
61. Xu, M., H. Lu, Y. H. Lee, Y. Wu, K. Liu, Y. Shi, H. An, J. Zhang, X. Wang, Y. Lai, and C. Dong. 2018. An interleukin-25-mediated autoregulatory circuit in keratinocytes plays a pivotal role in psoriatic skin inflammation. *Immunity* 48: 787–798.e4.
62. Karlsen, J. R., N. Borregaard, and J. B. Cowland. 2010. Induction of neutrophil gelatinase-associated lipocalin expression by co-stimulation with interleukin-17 and tumor necrosis factor-alpha is controlled by IkappaB-zeta but neither by C/EBP-beta nor C/EBP-delta. *J. Biol. Chem.* 285: 14088–14100.
63. Cowland, J. B., T. Muta, and N. Borregaard. 2006. IL-1beta-specific up-regulation of neutrophil gelatinase-associated lipocalin is controlled by IkappaB-zeta. *J. Immunol.* 176: 5559–5566.
64. Dobosz, E., M. Wilamowski, M. Lech, B. Bugara, J. Jura, J. Potempa, and J. Koziel. 2016. MCPIP-1, alias regnase-1, controls epithelial inflammation by posttranscriptional regulation of IL-8 production. *J. Innate Immun.* 8: 564–578.